COMPARISON OF HIGH ORDER METHODS FOR TRANSONIC INVISCID FLOWS

Jiří Holman, Jiří Fürst
Czech Technical University in Prague, Faculty of Mechanical Engineering, Department of Technical Mathematics

Introduction

This work presents the comparison of reconstruction methods for the spatial second order accurate scheme. We are considering widely used MUSCL reconstruction, which is implemented by analogy with one-dimensional reconstruction at three axis directions and so called weighted least square reconstruction (WLSQR), which is based on piecewise polynomial reconstruction similar to WENO scheme. These methods are applied in the finite volume framework to several cases of inviscid transonic flow.

Mathematical model and numerical solution

Inviscid flow is described by the system of Euler equations, which is closed by the equation of state for ideal gas:

$$\frac{\partial W}{\partial t} + \frac{\partial F}{\partial x} + \frac{\partial G}{\partial y} + \frac{\partial H}{\partial z} = 0 \tag{1}$$

$$p = (\kappa - 1)\left[e - \frac{1}{2}\rho(u^2 + v^2 + w^2)\right] \tag{2}$$

where $W = (\rho, \rho u, \rho v, \rho w, e)^T$ is vector, which contains unknown conservative variables and F, G, H are inviscid fluxes. System of Euler equations (1) is solved by the cell centered finite volume method, which can be written in semi-discrete form[1]

$$\frac{dW_i(t)}{dt} = -\frac{1}{|\Omega_i|} \sum_{k=1}^{6} \widehat{F}_k(W_i, W_j, \vec{n})\Delta S_k \tag{3}$$

$$\widehat{F} \approx (F, G, H) \cdot \vec{n} = Fn_x + Gn_y + Hn_z \tag{4}$$

where W_i is an averaged solution over i-cell Ω_i[2], ΔS is volume of interface between cells Ω_i and Ω_j and $\vec{n} = (n_x, n_y, n_z)$ is outer unit normal vector. $\widehat{F}$ is numerical flux, which is obtained by AUSM [8] or HLLC [1] scheme.
Set of ordinary differential equations (3) is then solved either by explicit multistage TVD Runge-Kutta method [6] or by the implicit backward Euler method [5].

---

[1]We are considering structured hexahedral H-type mesh.
[2]Computation domain is decomposed to the hexahedral sub-domains Ω_i (cells) with respect to $\Omega_i \cap \Omega_j = \varnothing$.

The reconstruction methods

Basic finite volume method[3] (3) is only first order accurate, which means that suffers from strong artificial dissipation. One of possible ways, how to overcome this problem is piecewise polynomial reconstruction from the cells averaged values. In our case, we use only linear reconstruction of second order accuracy, although it is possible to extend following methods to the higher order. High order finite volume method can be written as

$$\frac{dW_i(t)}{dt} = -\frac{1}{|\Omega_i|} \sum_{k=1}^{6} \widehat{F}_k(\widetilde{W}_i, \widetilde{W}_j, \vec{n}) \Delta S_k \tag{5}$$

Where piecewise constant data W_i and W_j are substituted by the reconstructed variables $\widetilde{W}_i$ and $\widetilde{W}_j$.

Slope limiters reconstruction

This is the standard version of well known MUSCL reconstruction (for $\kappa = -1$) with minmod limiter [7]. This method is applied in each axis direction as one-dimensional reconstruction:
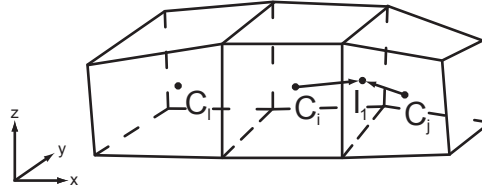
Figure 1: Schematic view on the mesh configuration

Let's indicate:

$$\overrightarrow{\delta_i} = \frac{W_j - W_i}{|C_i C_j|}, \qquad \overleftarrow{\delta_i} = \frac{W_i - W_l}{|C_i C_l|} \tag{6}$$

Then directional derivative in x-direction is computed as

$$\sigma_i^{(I_1)} = \mathbf{minmod}(\overrightarrow{\delta_i}, \overleftarrow{\delta_i}) \tag{7}$$

Reconstructed variables then can be written in the following form:

$$\widetilde{W}_i = W_i + |C_i I_1| \sigma_i^{(I_1)} \tag{8}$$
$$\widetilde{W}_j = W_j + |C_j I_1| \sigma_j^{(I_1)} \tag{9}$$

This reconstruction is analogously applied on the rest of interfaces. Note that while original one-dimensional reconstruction is TVD-type one, resulting scheme (5) with reconstructed data (8), (9) is not!

---

[3]In our case with AUSM or HLLC numerical flux.

Weighted Least Square Reconstruction (WLSQR)

Although above mentioned method is robust and keeps some of the good properties of TVD schemes, limiter function lower the accuracy near extremes and sometimes prevent the convergence to steady state. Another possibility is ENO/WENO type of reconstruction. Especially WENO reconstruction gives satisfactory results in both convergence to the steady state and sharp capture of extremes. Nevertheless, WENO procedure is complicated and computational efforts are relatively high. Therefore, more simple reconstruction procedure was introduced in [3].

Let's assume, that reconstruction should satisfy following requirements:

- **Conservativily constraint**

$$\int_{\Omega_i} P_i(\vec{x}; W) d\vec{x} = |\Omega_i| W_i \qquad (10)$$

   The mean value of interpolant $P_i(\vec{x}; W)$ over any cell Ω_i should be equal to cell average of W.

- **Accuracy**

$$\int_{\Omega_j} P_i(\vec{x}; W) d\vec{x} \approx |\Omega_j| W_j \qquad (11)$$

   Which means, that interpolant $P_i(\vec{x}; W)$ should satisfy (11) for cells Ω_j neighbouring with cell Ω_i.

- **Non-oscillatory**

   The total variation of intarpolant $P_i(\vec{x}; W)$ should be bounded for $h \rightarrow 0$, where h is characteristical mesh size.

Interpolant $P_i(\vec{x}; W)$ is obtained by minimizing error in (11) with respect to (10). It is well known, that this system leads to an unstable scheme. This problem can be solved by introducing non-linear weights, which is the key point of WLSQR method. It means, that interpolant $P_i(\vec{x}; W)$ is obtained by solving system:

$$\min \sum_{j \in \mathcal{M}_i} \left[w_{ij} \left(\int_{\Omega_j} P_i(\vec{x}; W) d\vec{x} - |\Omega_j| W_j \right) \right]^2, \quad \int_{\Omega_i} P_i(\vec{x}; W) d\vec{x} = |\Omega_i| W_i \qquad (12)$$

Where $\mathcal{M}_i$ is stencil, which contains cells Ω_j neighbouring with cell Ω_i and $w_{ij} > 0$ are weights, which depends on the solution W_i, W_j. The weights should be high, when W is smooth and small, when W is discontinuous. They can be chosen in the similar way as in WENO procedure [2]. In our case, we use weights introduced in [4], which are designed especially for WLSQR reconstruction:

$$w_{ij} = \frac{\alpha_{ij}}{\sum_{j \in \mathcal{M}_i} \alpha_{ij}}, \quad \alpha_{ij} = \sqrt{\frac{h^{-r}}{\left| \frac{W_i - W_j}{h} \right|^p + h^q}} \qquad (13)$$

According to [4], exponents p, q, r can be chosen as $p = 4, q = -2... - 3, r = 3$.
Sometimes it is possible to use simplified computation of weights:

$$w_{ij} = \frac{\alpha_{ij}}{\sum_{j \in \mathcal{M}_i} \alpha_{ij}}, \qquad \alpha_{ij} = \sqrt{\frac{h^{-r}}{\left| \frac{p_i - p_j}{h} \right|^p + h^q}} \tag{14}$$

Where we used pressure instead of corresponding component of W. Weights (14) are then
applied to all components of W. This simplification is used in this work.
Reconstructed variables are obtained as:

$$\widetilde{W}_i = P_i(\vec{x}_k, W), \qquad \widetilde{W}_j = P_j(\vec{x}_k, W) \tag{15}$$

Where $\vec{x}_k$ is center of gravity of the interface between cells Ω_i and Ω_j.

Transonic flow through the 3D test channel

First application of above described methods is transonic inviscid flow through the test channel.
This is the case of well know GAMM channel (2D test channel with circular bump with 10%
high), which is extended to 3D. The GAMM channel is used by many authors for validation.
Our goal in this section is the comparison of 2D and 3D calculation, which should be undistin-
guishable.
Problem was solved on structured H-type mesh with $185 \times 35 \times 12$ cells on the computational
domain fig. 2(a).

(a) 3D GAMM channel (2D geometry)   (b) Computational mesh for 3D GAMM channel
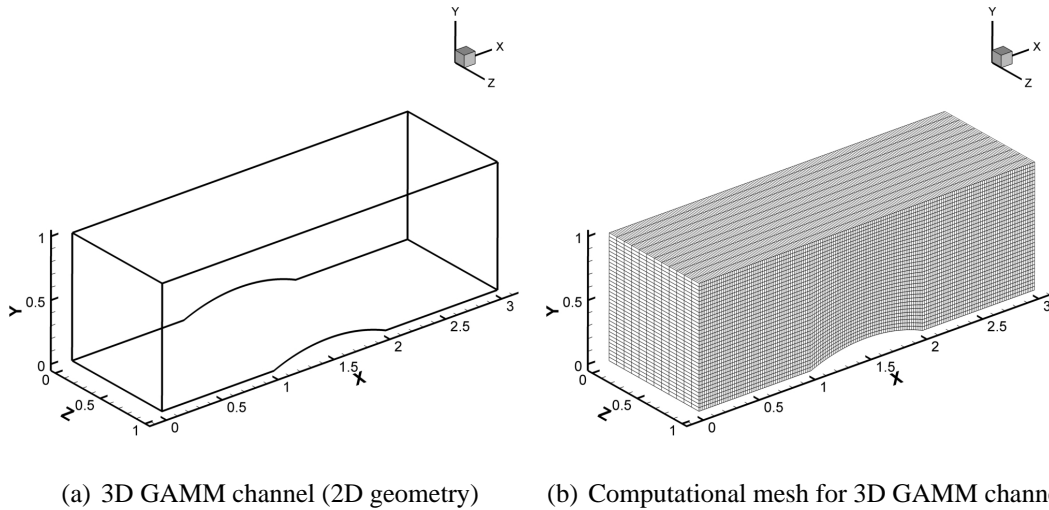
Figure 2: Computational domain and mesh for the flow through the 3D GAMM channel

We considered the configuration with the ratio of outlet static pressure and inlet stagnation
pressure set to $p_2/p_0 = 0.737$ and inlet angle to $\alpha_\infty = 0°$.

(a) MUSCL HLLC   (b) WLSQR HLLC
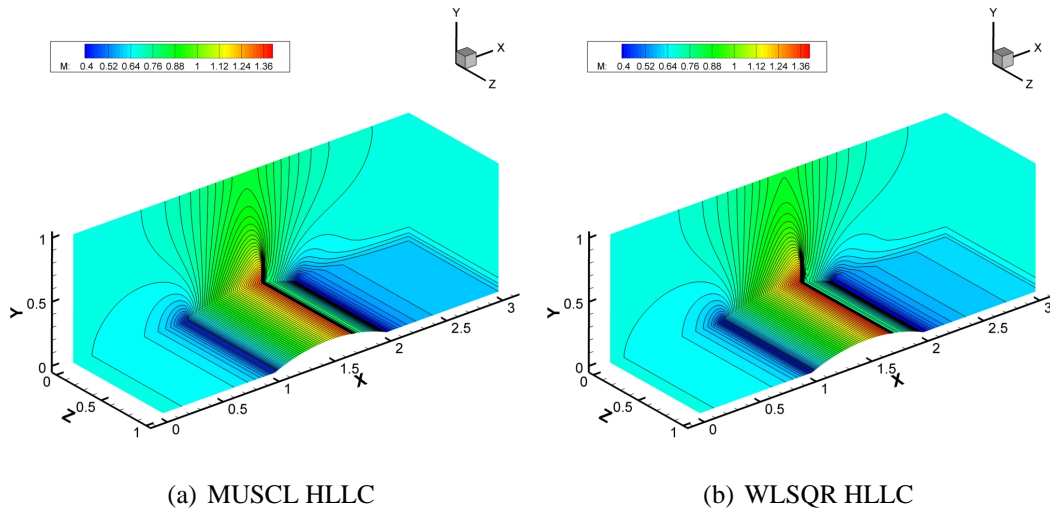
Figure 3: Comparison of Mach number isolines for the flow through the 3D GAMM channel
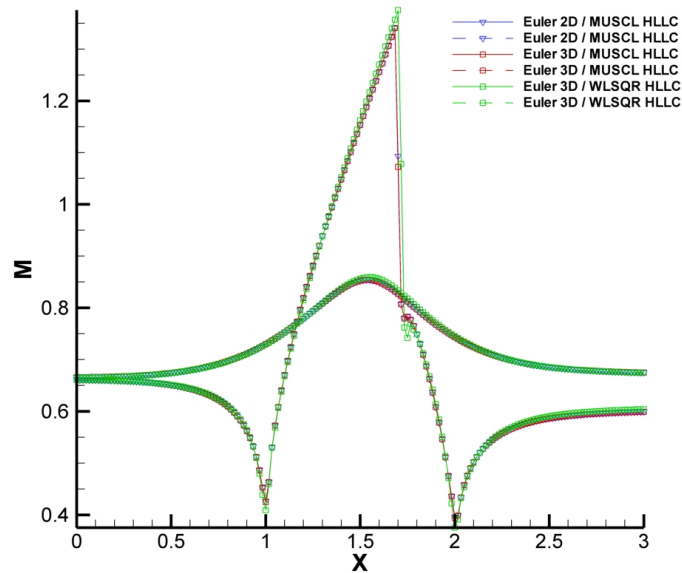
Figure 4: Comparison of Mach number distributions on the upper and lower wall of the 3D GAMM channel

From fig. 4 is clear, that we obtain almost the same results from the 2D and 3D calculation. The WLSQR scheme gives slightly higher maximum of Mach number and sharper Zierep singularity. From fig. 3 one can see, that both schemes performed very similar in this case.

Transonic flow around the NACA 0012 wing

Next application is transonic inviscid flow around the NACA 0012 wing. We solved transonic regime with $M_\infty = 0.85$ and $\alpha_\infty = 0°$ on the domain fig. 5(a)[4] , which was covered by structured H-type mesh with $100 \times 50 \times 25$ cells.

(a) Computational domain

(b) Detail of mesh in the area around the NACA 0012 wing
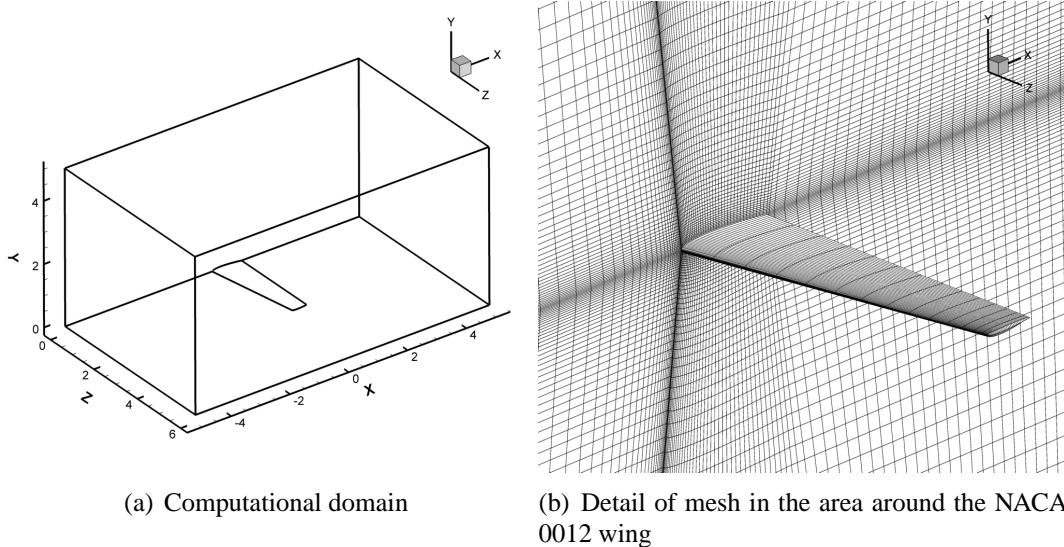
Figure 5: Computational domain and mesh for the flow around the NACA 0012 wing

From the following figures we can see, that both schemes archived almost the same results. Again, WLSQR scheme gives slightly higher maximum values of pressure coefficient.

(a) MUSCL HLLC

(b) WLSQR AUSM
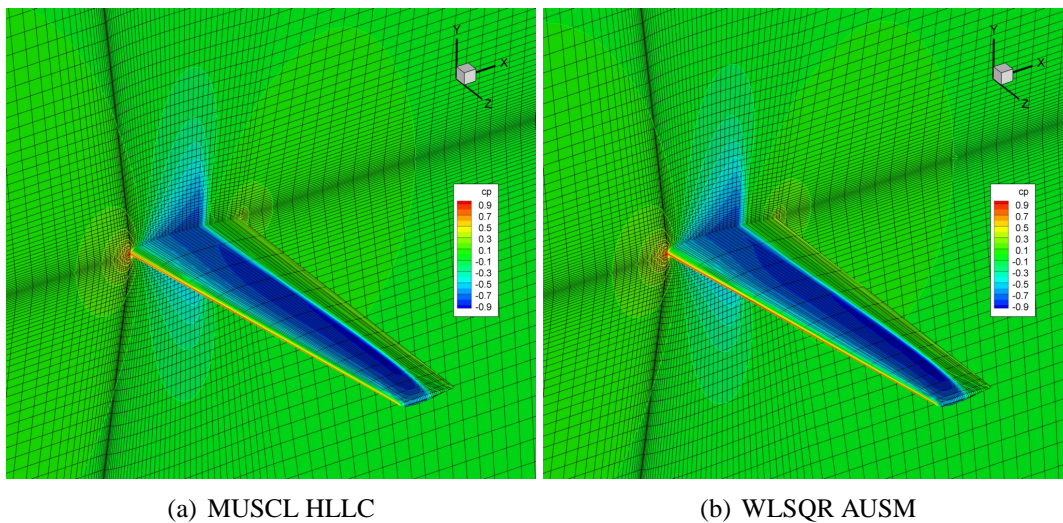
Figure 6: Comparison of pressure coefficient isolines for the flow around the NACA 0012 wing

---

[4]Because angle of attack is set to zero, we can solve only one half of the real domain.
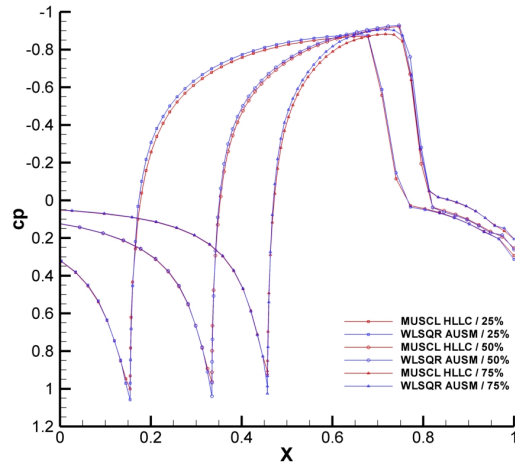
Figure 7: Comparison of pressure coefficient distributions in three cuts of NACA 0012 wing

Transonic flow through the 3D turbine cascade

The last application is transonic inviscid flow through the SE-3D1 turbine cascade. We assume that the flow is periodic from blade to blade and therefore we can solve only one period. Computational domain was discretized by the structured H-type mesh with $90 \times 24 \times 17$ cells (fig. 8).
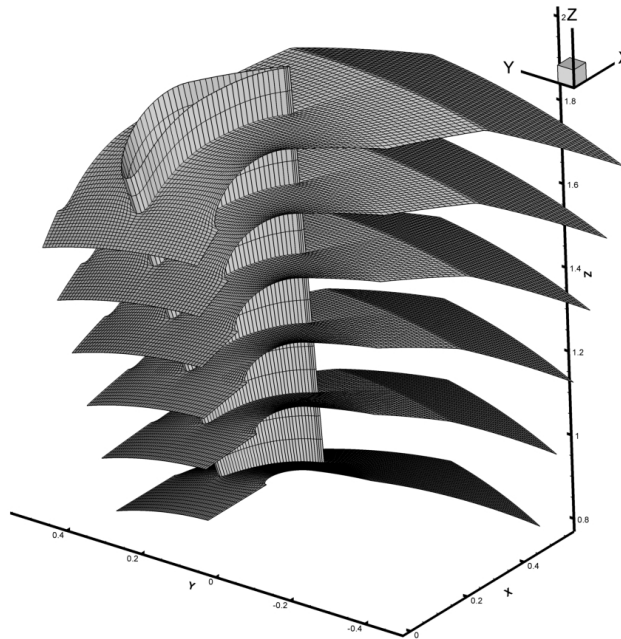
Figure 8: Computational mesh for the flow through the SE-3D1 turbine cascade

Inlet and outlet conditions depends on the radius, see [5].

(a) MUSCL HLLC   (b) WLSQR HLLC
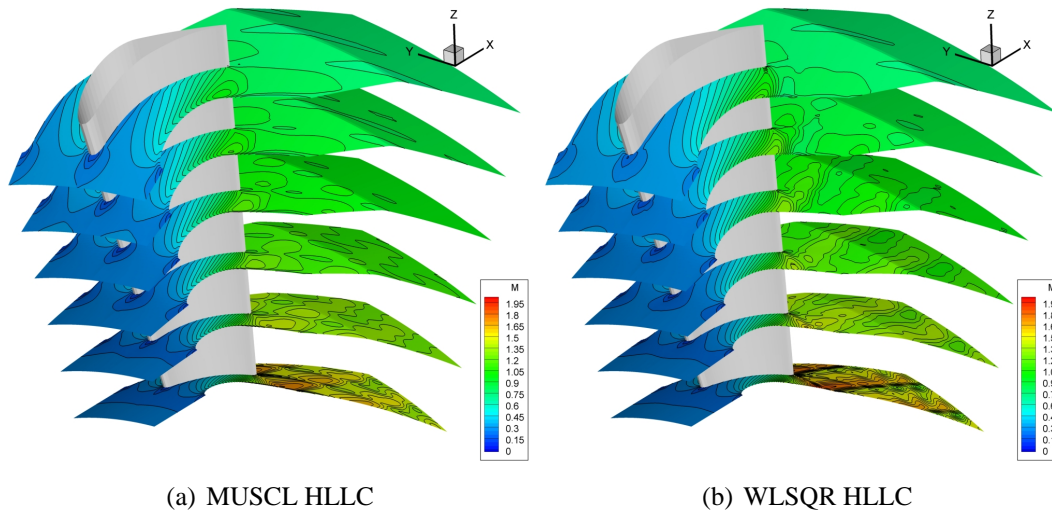
Figure 9: Comparison of Mach number isolines for the flow through the SE-3D1 turbine cascade
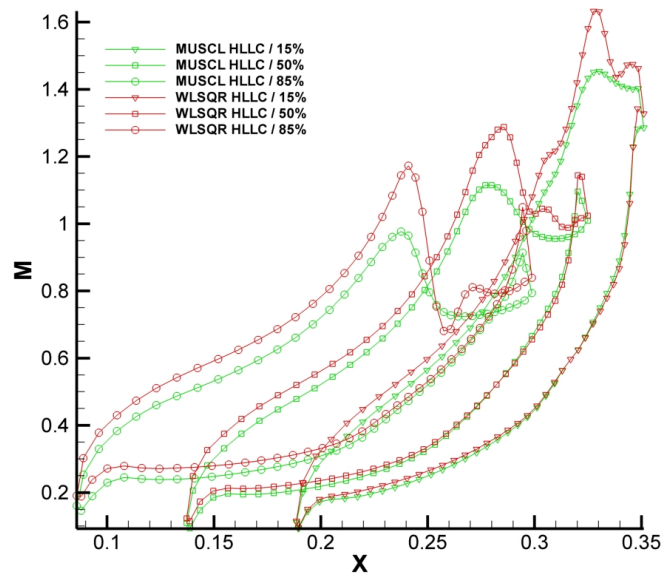
Figure 10: Comparison of Mach number distributions along the blade in three cuts

From the figure 9 one can see, that WLSQR scheme archived much better resolution of the shockwaves. MUSCL scheme gives all shockwaves smeared and moreover failed to capture second part of shockwave. From figure 10 we can see relatively large difference between the

WLSQR and MUSCL schemes (especially maximal values of Mach number), which corresponds to the trend from previous sections.

Conclusions

We described two different approaches for developing high order finite volume scheme. MUSCL reconstruction is very simple, robust and computationally low-cost. On the regular meshes (or meshes, that are close to be regular) gives satisfactory results. Nevertheless, on the high curved grids fails to capture shockwaves or other extremes due to limiter function, which lower the accuracy to the first order in theirs vicinity and due to one-dimensional construction.

The WLSQR reconstruction is clearly superior over the MUSCL reconstruction. In performs similar or slightly better on regular grids and much better on the coarse curved grids due to multidimensional reconstruction approach and absence of limiter function. On the other hand, it is computationally more demanding and allows arise small oscillations (especially in the high supersonic regimes).

References

[1] Batten, P., Leschziner, M. A., Goldberg, U. C.: Average-State Jacobians and Implicit Methods for Compressible Viscous and Turbulent Flows, Journal of computational physics 137, 1997

[2] Friedrich, O.: Weighted Essentially Non-Oscillatory Schemes for the Interpolation of Mean Values on Unstructured Grids, Journal of computational physics 144, 1998

[3] Fürst, J., Kozel, K.: Second and Third Order Weighted ENO Scheme on Unstructured Meshes, Finite volumes for complex applications, 2002

[4] Fürst, J.: A Finite Volume Scheme with Weighted Least Square Reconstruction, Finite volumes for complex applications IV, 2005

[5] Fürst, J.: Numerical Solution of Compressible Flows Using TVD and ENO Finite Volume Methods, Habilitation thesis CTU in Prague, Faculty of Mechanical Engineering, 2004

[6] Holman, J.:Numerical Solution of Compressible Turbulent Flows in External and Internal Aerodynamics, Diploma thesis CTU in Prague, Faculty of Mechanical Engineering, 2007 (in czech)

[7] Kozel, K., Fürst, J.: Numerical Solution of Flow Problems I, Scriptum CTU in Prague, Faculty of Mechanical Engineering, 2001 (in czech)

[8] Liou, M. S.: Ten Years in the Making-AUSM-family, NASA/TM-2001-210977, 2001